Cell Tissue Res (2013) 352:149–159
DOI 10.1007/s00441-013-1580-3

REVIEW

Insights into cell-to-cell and cell-to-blood-vessel communications in the brain: in vivo multiphoton microscopy

Matthias Osswald · Frank Winkler

Received: 18 December 2012 / Accepted: 31 January 2013 / Published online: 26 February 2013

Abstract A complex and reciprocal communication of cells with each other and with relevant parts of the tissue stroma governs many biological processes in both health and disease. However, in the past, the study of these anatomical and molecular interactions has suffered from a lack of appropriate experimental models. An imaging methodology aimed at changing this should allow intravital display and quantification in an intact non-traumatized organ, imaging over a wide range of time spans including extended periods (i.e., months), many repetitive measurements of the same cell or area to permit the study of the cause and consequence of biological processes, the display of various cell types and their reciprocal interaction with each other in three dimensions, the co-registration of relevant physiological parameters and reporters for selected molecular pathways and as high as possible resolution to visualize subcellular structures such as organelles. Remarkably, intravital multiphoton microscopy (in vivo MPLSM) through a chronic cranial window allows us to do all these things, making the brain the inner organ of choice for this technology. Here, we give an overview of the application of in vivo MPLSM to study the choreography of cellular, vascular and molecular interactions in the healthy brain and in neurological diseases. We focus on brain tumor formation, progression and response to therapies. This review further aims at demonstrating that we stand at the beginning of full exploitation of the opportunities provided by this technology and gives clues to future directions that appear most promising.

Keywords Multiphoton microscopy · Two-photon microscopy · Cancer · Neuroscience · Brain

Introduction

The reciprocal interaction of cells with each other and the function of cellular networks, embedded in an adequate anatomical, physiological and molecular environment are impossible to recapitulate in vitro. Therefore, many in vitro findings in biomedical research cannot be confirmed in animal experiments or even in clinical trials. One of many examples for this is the finding of an extremely low overlap of genes that drive fast glioma migration in vitro with those genes that do the same in vivo (4.2%; Tatenhorst et al. 2005). Although the ease of manipulation is a great advantage for in vitro studies and a principal cellular mechanisms can be readily studied in a meaningful way, the shortcomings of *ex vivo* research increase to an alarming level when complex interactions between cell types, the mechanisms of disease progression and responses to therapies are of interest.

All this argues for the investigation of cells and tissues in their natural environment, namely in a live organism. In vivo studies, however, have long suffered from the limitation that microscopy, which is required for cytological studies because of its high resolution, can penetrate only a few microns into living tissues. In the 19th century, blood flow was examined in the thin ears of small animals by means of the first transilluminational intravital imaging studies and later metastasis formation was similarly followed in the blood vessels of rabbit ears (Wood 1958). However, such a method fails to reach areas beyond the

Electronic supplementary material The online version of this article (doi:10.1007/s00441-013-1580-3) contains supplementary material, which is available to authorized users.

M. Osswald · F. Winkler (✉)
Department of Neurooncology, Neurology Clinic and National Center for Tumor Diseases, University of Heidelberg and German Cancer Research Center (DKFZ), Heidelberg, Germany
e-mail: frank.winkler@med.uni-heidelberg.de

surface of inner organs in which the region of interest lies for most biological questions. Researchers have therefore removed organs and cut them into thin slices, allowing high-resolution imaging of tissue transections with standard histological methods, immunostaining, in situ hybridization, or electron microscopy. Unfortunately, this solution to the problem has the great shortcoming that an observed phenomenon cannot be followed over time, allowing only hypotheses to be made about the cause and consequence of what is seen. This excessively limits the study of cells in health and disease.

To overcome these limitations, multiphoton microscopy (multiphoton laser scanning microscopy [MPLSM], two-photon microscopy) was introduced in 1990 for application in biological systems (Denk et al. 1990). For the first time, high-resolution images of structures could be obtained in live tissue to a depth of up to 1000 μm (Brown et al. 2001) and this, most importantly, without causing relevant photodamage that would compromise both the interpretation of the results and repetetive imaging over time. Therefore, MPLSM has experienced a dramatic increase in usage over the last 20 years in neuroscience and beyond. From our point of view, its possibilities have by no means been fully explored as yet and technological challenges remain. Today, the opportunity to buy multiphoton microscopes and lasers from various companies in a more or less "ready-to-use" set-up gives the false impression that intravital MPLSM is straightforward and easy to establish in every laboratory. This review aims at bringing together the physical, technological, biological and medical aspects of in vivo MPLSM of the brain, with the aim of pointing out technical solutions, unexpected opportunities and unprecedented insights that can be gained with this methodology. We hope that this will help the reader to appreciate more fully the promises and pitfalls of this technology and to improve interpretations of the results so obtained.

Advantages of MPLSM and new technical developments

Traditional optical microscope techniques use linear (one photon) absorption for excitation, which results in strong light scattering in deeper tissues (Helmchen and Denk 2005). This also affects confocal microscopy, which achieves three-dimensional (3D) resolution with a detection pinhole, strongly reducing signal strength in the depth of the tissue. Therefore, the use of confocal microscopy is extremely limited when it comes to in vivo applications: out-of-focus excitation and the high powers necessary to achieve in-focus excitation make its use for imaging below 10–20 μm in living tissues nearly impossible because of the exorbitant photoxocity that would result. Compared with one photon excitation or confocal imaging, MPLSM shows much lower phototoxicity and thereby less interference in biological processes, an important prerequisite for long-term imaging (Squirrell et al. 1999).

Non-linear optical microscopy techniques are fundamentally different in that they use "higher-order" light-matter interactions involving multiple photons for contrast generation (Denk et al. 1990; Helmchen and Denk 2005). In MPLSM, two (or more) photons that arrive simultaneously at a molecule combine their energies to promote the molecule to an excited state, which then generates normal fluorescence emission. To generate a signal of sufficient intensity, excitation has to be concentrated in space and time; for space, an objective with a high numerical aperture (N/A) is required, whereas for time, a special laser system that emits ultrashort (less than a picosecond) pulses with high peak intensities is needed. The efficiency of multiphoton excitation also depends on the physical absorption properties of the molecule ("multiphoton absorption cross-section"), which is not easy to predict from the one-photon properties of the same fluorophore and has to be tested for multiphoton excitation at various wavelengths. As a rule of thumb, the optimal excitation wavelength for two-photon excitation is slightly lower than twice the wavelength used for optimal one-photon excitation. All in all, the two-photon absorption spectra of a given fluorophore tend to be unpredictable, as seen with most red fluorescent protein (RFP) variants, where two absorption peaks are present: between 1,000 and 1,100 nm and below 800 nm (Drobizhev et al. 2011).

The physics of multiphoton excitation has many advantages that make it the method of choice for intravital imaging: (1) excitation is achieved with high-wavelength photons of low energy that can penetrate much deeper into biological tissues without inflicting photodamage (see below); (2) excitation and emission wavelengths are markedly separated, making simultaneous excitation and emission and multicolor imaging much easier; (3) multiphoton excitation is confined to an extremely small volume, i.e., the perifocal region determined by the objective, which is in contrast to confocal microscopy during which absorption occurs in the entire excitation light cone (Denk et al. 1990). This high spacial selectivity of excitation makes it possible to reduce phototoxicity to a minimum and also to collect all light coming out of the tissue without a pinhole, greatly increasing the sensitivity of the method. It also allows the laser beam to be used as a micro-manipulator, since femtoliter volumes can be selectively targeted: this facility has been used for selective photo-occlusion of cerebral capillaries (Nimmerjahn et al. 2005), ablation of single cells within an anatomical or functional network (Davalos et al. 2005; Fig. 1, Supplementary video 1), photobleaching and photolytic release of caged compounds (Dakin and Li 2006;

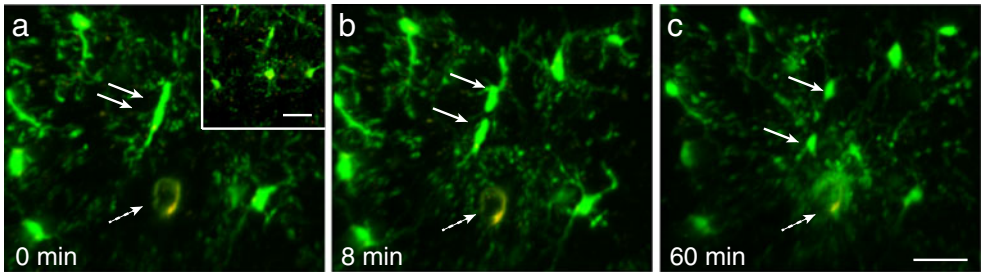

Fig. 1 Microglia form a highly active patrol in the living mouse brain. After laser-induced necrosis of one single microglial cell (*dotted arrow* in **a–c**, also shown in *center* of *inset* before laser treatment), the neighboring cells rapidly send protrusions to the dead cell, which is completely encapsulated by the protrusions over 1 h (see also Supplementary video 1). One cell divides and one daughter cell migrates in the direction of the dead cell (*arrows*). The microglia cells were labeled by green fluorescent protein (GFP) expression in a CX3CR1-GFP animal. MPLSM images were acquired through a chronic cranial window (M. Osswald, unpublished). *Bars* 30 μm. For video sequence, see Supplementary video 1

Kantevari et al. 2010; Svoboda et al. 1996). All in all, the main strength of MPLSM is its ability to maintain resolution and contrast within scattering tissue without relevant photodamage, thereby allowing the observation of cells in their normal environment.

As previously mentioned, two-photon excitation produces less photodamage than other imaging techniques (Squirrell et al. 1999). To attain a minimum of toxicity, laser power should be as low as possible. The required power is defined by various parameters, e.g., window quality, brightness of the fluorophore, depth and nature of the structure of interest, or technical parameters such as detector sensitivity. A line scan produces much less photodamage than a frame scan. As an example, for the imaging of a 3D stack of a normal fluorescein isothiocyanate (FITC) angiogram (600×600×600 μm, excited with a wavelength of 750 nm, maximum laser power 3,319 mW), we need, with our set-up, approximately 200 mW (6% laser power) at the brain surface, 330 mW (10%) at −100 μm, 430 mW (13%) at −200 μm, 660 mW (20%) at −300 μm, 930 mW (28%) at −400 μm and 1330 mW (40%) at −500 μm (where the negative length signifies the depth into the tissue). After laser power, the scan speed is the second variable defining phototoxicity: the faster the speed, the lower the toxicity. For the same image quality, you might need a slower scan speed in deep brain regions compared with superficial brain regions. Concerning thermal damage, an advantage of brain imaging is strong blood perfusion, which ensures good thermal convection and thereby offers the opportunity to image one brain region over a long time period (see below). Nevertheless, it is of crucial importance to continuously check for any indications for phototoxicity, optimally in prior establishing experiments. For acute imaging, photoxicity can be detected by a reduction of blood flow, final stasis in microvessels, or even blood vessel rupture. In chronic (repetitive) imaging, the following specific changes of the scanned tissue volume have to be carefully sought, when compared with surrounding tissue: increase in background signal, rarification of blood vessels, change of cellular morphology and reduction of image quality. If any of these occur, the experiment has to be terminated, since relevant phototoxicity that will strongly interfere with interpretation of the results has taken place. Careful imaging and reduction of laser power to a minimum (see above) prevents significant phototoxicity.

These physical advantages of MPLSM have helped to inspire the development of exciting fluorescent marker and reporter technologies (see below). In turn, further technical advances have recently been made in the "hardware". In short, three major advances have been made in the last few years. First, a great increase in detector sensitivity (e.g., with GaAsP detectors) has been achieved, which permits imaging into greater depths (up to 800–1000 μm in the living mouse brain) with lower excitation power. Second, optical parametric oscillators have been introduced into the laser technology enabling the extension of the excitation range from near-infrared to infrared (for a review, see Niesner and Hauser 2011). Now, far-red dyes can be excited and higher wavelengths further increase depth penetration and resolution. Limitations are the lower maximum laser powers of current systems and the paucity of genetic fluorophores in this range. Third, the development of novel endoscopy techniques by using thin (ca. 500 μm) micro-optical probes allows access to regions millimeters beyond the surface, as shown for deep brain regions such as the hippocampus (Barretto et al. 2011).

A chronic window into the live brain—in three dimensions

Long-term intravital microscopy of an intact organ is mainly restricted to the skin and the brain, since these two are repetitively accessible through chronic windows without the need to traumatize the tissue. Other window technologies, e.g., the mammary window (Kedrin et al. 2008), seem to be difficult to maintain over several days. The dorsal skinfold chamber can be maintained over 3–4 weeks and

has allowed insights into various aspects of microcirculation, the progression of cancer in the skin and the response to therapies (Tong et al. 2004; Yuan et al. 1996). Although this might one day change with new endoscopy techniques, the cranial window is, at the moment, the only technology that allows us to image a large volume of an intact inner organ for prolonged time spans, i.e., for many months (Fuhrmann et al. 2007) up to 1 year and more (M. Osswald, F. Winkler, personal observation), without a significant reduction of imaging quality. In addition and of utmost importance for intravital microscopy, breathing artefacts can be reduced to zero by various fixation devices that take advantage of the stable anatomical structure of the skull and heartbeat artefacts are also negligible in the cranial cavity (Hefendehl et al. 2011). For short-term experiments, an acute cranial window can be used whereby agar is placed between a cover-glass and the brain and parallel electrophysiological recordings are possible (Helmchen and Denk 2005). Access to the brain is also possible by thinning the skull over the brain (Xu et al. 2007) but this has to be carried out repeatedly, since the bone reheals and the field of view is once more restricted.

In contrast, the chronic cranial window replaces a larger skull flap with a thin glass window that is permanently glued to the surrounding bone over its whole circumference, allowing the imaging of larger areas of the mouse cerebrum. This window can in principle also be extended backwards to image the mouse cerebellum (M. Osswald, unpublished). The area that can be examined with a chronic cranial window is a circle as large as 6×6 mm in our laboratory (Kienast et al. 2010; von Baumgarten et al. 2011; Yuan et al. 1994) allowing large upper parts of both cerebral hemispheres to be imaged. After preparation, a recovery period of 3–4 weeks should be undertaken before experimentation starts, to allow any microglial and astrocytic activation to settle down (own observation), as this also affects the morphology of dendritic spines (Xu et al. 2007).

One further strength of the technology is the opportunity to collect data over highly diverse time spans. This allows the researcher to adapt to the speed of the biological process observed. Blood flow in cerebral capillaries is extremely fast and its speed can be measured by line scans of up to 500 Hz (Chae et al. 2010; von Baumgarten et al. 2011). Indeed, technological advances have been made in the last few years to allow the high-speed imaging of cellular networks with near-millisecond precision (Gobel et al. 2007; Grewe et al. 2010). Migration of single cells and their interaction with other cells occurs on the scale of minutes to hours to days; these time spans have been successfully applied to attain unprecedented insight into immune cell interactions (Bartholomaus et al. 2009; Kawakami et al. 2005), glioma cell migration (Winkler et al. 2009) and microglia activity (Nimmerjahn et al. 2005). Other processes take weeks to months, such as neuronal degeneration and changes of spine morphology (Fuhrmann et al. 2007; Xu et al. 2007) and the formation and evolution of brain metastases (Kienast et al. 2010). Therefore, experimental conditions have to be carefully selected in advance with respect to the expected kinetics of the process of interest. The major limiting factor is the well-being of the animal, which has to be maintained with great care when long-term imaging is required. Therefore, in our experience, image acquisition with the necessary anesthesia of the animal and reduction in potential photodamage to the brain (see above) can be achieved under the following general experimental conditions: during continuous anesthesia (preferably by inhalation) over minutes to a maximum of 2–3 h; every 12 h for 2–3 days; every 24 h for up to 5 days; every 3 days for weeks; or every 7 days for many months.

The re-identification of the same area under the window over long periods of time is straightforward and merely takes a few seconds. Hence, a small marker is set next to the window region and serves as a reference for an electronic stage holder. Fine tuning is performed by orientation via superficial blood vessels or neurons, which remain stable over months in the normal brain.

For the study of cell morphology and cell–cell and cell–blood-vessel interactions, the recording of a 3D tissue volume (Supplementary videos 1, 2) is not only “nice to have” but also often of paramount importance. This cannot be stressed enough and the opportunity to image a z-stack in high z-resolution with single images every 1–3 μm is one of the major advantages of in vivo MPLSM. These images can later be assembled for 3D reconstruction, optimally by taking advantage of advanced software that is available today that allows the image stack to be displayed and quantified in three dimensions. Those software solutions also enable fragmentation, fiber tracking and object tracking by integration of the fourth dimension, i.e., time, into the analysis.

Simultaneous multiparameter imaging

Modern in vivo MPLSM set-ups allow the collection of up to four or more channels in parallel. With the use of appropriate filters, these channels can be employed to study several parameters in parallel. Furthermore, the most common Ti:Saphire two-photon lasers are continuously tunable between around 700 to 1050 nm, enabling the excitation of most blue to near-red fluorophores with the excitation wavelength of choice. This is an additional advantage that can be used to increase further the number of channels that are collected and thereby the information that can be retrieved. Even two different green colors can be separated by this, e.g., FITC can be readily excited at 750 nm, whereas GFP cannot, as the maximum for GFP is between 850 and

880 nm. By using these different excitation wavelengths and by collecting the images subsequently, followed by electronic unmixing strategies, the green channel can be used to collect two different pieces of information. Another advantage of two-photon microscopy is the fact that most RFP variants can be effectively excited below 700 nm (Drobizhev et al. 2011), allowing the simultaneous excitation of green and red fluorophores and the collection of emissions with two filter sets, saving acquisition time.

Labeling of cells, organelles and physiological and molecular parameters

For fluorescence imaging, structures of interest need to be labeled, unless they are autofluorescent (Table 1). In the brain, intrinsic fluorescence is mostly attributable to fluctuations of reduced nicotinamide adenine dinucleotide. Nevertheless, this can be used to measure hypoxia and the metabolic state of cells and its temporal change is cell-type-specific (Kasischke et al. 2004, 2011; Takano et al. 2007b). The signal generated by second harmonic generation (Brown et al. 2003) is also label-free but usually requires types of collagen fibres that are not present in the brain parenchyma, although they can be used to image the meninges.

In vivo labeling techniques for staining cells in living tissues have greatly advanced. In the intact brain, various cell types (to date, mainly astrocytes, microglia, neurons and endothelial cells) have been visualized in their natural habitat (1) by brain-superficial application of vital dyes that are either selectively uptaken by the respective cell types or inserted cell-type-specifically by (2) microinjection or (3) iontophoretic application. If a chronic cranial window is used, this can be removed for the application of dyes and later re-glued into position; alternatively, we have developed a tubing system that is permanently glued between the window and skull that allows repetitive application of agents without the need to remove the window (M. Osswald, unpublished). As one example, locally applied sulforhodamine 101 (SR101) is selectively uptaken by astrocytes (Nimmerjahn et al. 2004; Fig. 2, Supplementary video 3). SR101 can be locally applied on the brain surface to label the whole astrocytic network to a depth of 800 μm (own experience). Other lipophilic substances that can be supplied superficially and are uptaken by astrocytes are the various calcium sensors, e.g., the Ca^{2+} indicator fluo-4 AM (acetoxymethylester of fluo-4; Gee et al. 2000; Wang et al. 2006; Fig. 3, Supplementary video 4, see below). Microinjection, bulk-loading, or electroporation of vital dyes suffers from the invasive character of the labeling techniques but offers the chance to label selected cells exclusively and to study, for example, neuronal circuits (Nagayama et al. 2007). Since the availability of fluorescent markers for all kinds of cellular functions is rapidly increasing, the researcher can today select from a wide array of agents that fit his experimental needs. Of note, chemical dyes can be used to monitor

Table 1 Fluorescence labeling methods for in vivo multiphoton laser scanning microscopy of the brain

Method	Examples of fluorophores	Function/labeling of cell/structure	Recommended references
Application of fluorescent dyes			
Local cortical application	Sulforhodamine 101	Astrocytes	Nimmerjahn et al. 2004
	Calcium dyes (e.g., FLUO-4 AM, Oregon Green 488 BAPTA-1)	Calcium communication in astrocytes, neurons	Gee et al. 2000; Wang et al. 2006; Nagayama et al. 2007
Ex vivo cell labeling	Cell retention dyes, LysoTracker/ MitoTracker	Cell division rate, senescence, cell organelles	
Intravenous injection	Fluorescently labeled dextrans (FITC, TRITC)	Blood vessel staining, blood flow velocity, microvascular permeability	Brown et al. 2001; Kienast et al. 2010; Chae et al. 2010; von Baumgarten et al. 2011
	Fluorescent apoptotic tracer	visualisation of apoptosis	
	Fluorescently labeled antibodies	cell adhesion molecules	Sipkins et al. 2005
Genetic insertion of fluorescent proteins			
Use of genetic mouse models	(CX3CR1-)GFP	Microglia	Jung et al. 2000; Nimmerjahn et al., 2005
	(GFAP-)GFP	Astrocytes	Nolte et al. 2001; Nimmerjahn et al. 2004
	(THY-1-)YFP	Neurons	Feng et al. 2000; Fuhrmann et al. 2010
	(Tie-2-)GFP	Endothelium	Motoike et al. 2000; Kienast et al. 2010
Cortical injection of lentivirus	GFP and many other fluorophores[a]	Neurons	Dittgen et al. 2004
Ex vivo cell transfection of cells	Many fluorescent proteins in many cell types[a]	Cytoplasmic expression	Kienast et al. 2010
		Nucleic expression	Yamauchi et al. 2006

[a] Coral fluorescent proteins and their derivatives

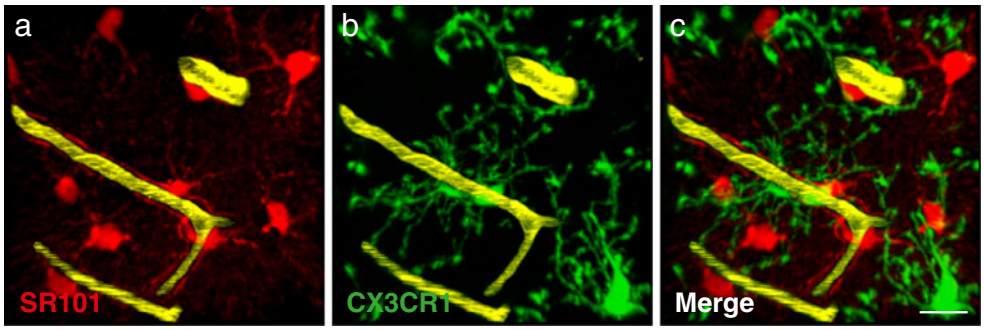

Fig. 2 Astrocyte and microglia interaction. Two types of glia cells can be simultaneously imaged by using sulforhodamine 101 (*SR101*) for the detection of astrocytes (*red* in **a**, **c**) and transgenic CX3CR1-GFP-mice for tracking microglia (*green* in **b**, **c**). Blood vessels are shown in *yellow*. M. Osswald, unpublished. *Bar* 15 μm. For video sequence, see Supplementary video 3

cells for days only, since fluorescence decreases by photobleaching and is diluted during cell division.

Another way of tracking cells offers the ability to follow specific cells long-term; this is achieved by the stable genetic insertion of fluorophores controlled by promotors specific for glial, neuronal, or other cell types. The availability of transgenic mouse models with fluorescently labeled (subsets of) cells is rapidly growing. In the following, we will give a short overview of the frequently used mouse models in neuroscience; another area in which many of these cell-type-specific models are available is immunology (for a review involving MPLSM, see Niesner and Hauser 2011). One common transgenic model to track microglial cells is the CX3CR1-GFP mouse in which enhanced GFP (EGFP) has been placed into the Cx3cr1 locus (Jung et al. 2000; Nimmerjahn et al. 2005; Figs. 1, 2, Supplementary videos 1, 3). In mice bearing one mutated allele, the Cx3cr1-bearing cells (in the healthy brain, microglial cells) still have a function for this receptor, whereas in homozygous mice, the chemokine receptor is totally replaced by EGFP and the function is lost (Fuhrmann et al. 2010). Neurons (e.g., in Thy-1-YFP mice; Feng et al. 2000; Fuhrmann et al. 2010), astrocytes (e.g., in GFAP-GFP mice; Nimmerjahn et al. 2004; Nolte et al. 2001) and other cell types (e.g., endothelium in Tie-2-GFP mice; Motoike et al. 2000) can also be studied in transgenic mice. Furthermore, cell organelles such as mitochondria (Misgeld et al. 2007) can be selectively studied in newly developed transgenic animals. A great advantage of transgenic mouse models is the non-invasive long-term labeling of well-defined cells/organelles and the opportunity to make a knock-in or knock-out of a gene visible. Furthermore, these animals can be cross-bred with these bearing genetic alterations for specific disease models (Fuhrmann et al. 2007). Another genetic approach to label

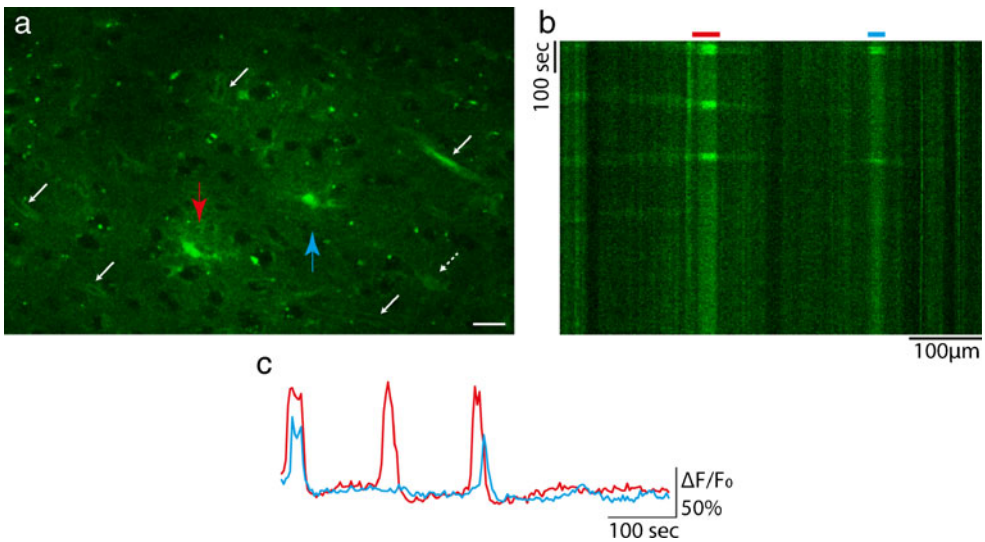

Fig. 3 Calcium imaging. Imaging of astrocytic calcium waves by using direct cortical application of the calcium indicator fluo-4 AM. **a** Two neighboring astrocytes (*red arrow*, *blue arrow*) show a bright fluorescence signal reflecting an increase in $[Ca]_i$. Another astrocyte (*dotted white arrow*) shows no $[Ca]_i$ increase. The change of $[Ca]_i$ of the two activated astrocytes (*red arrow*, *blue arrow* in **a**) over time is shown in **b** (kymograph illustrating the calcium increase in the two marked astrocytes on the *x*-axis over time shown on the *y*-axis) and **c** (*red line*, *blue line*, respectively). The direction of the wave(s) is from the *red* to the *blue* astrocyte. In addition, the astrocytic endfeet forming the blood-brain barrier are visible in **a** (*white arrows*). M. Osswald, unpublished. *Bars* 20 μm. For video sequence, see Supplementary video 4

brain cells selectively and to visualize certain cell functions is the cortical injection of a lentivirus in terms of the gene transfer technique, e.g., lentivirus-based EGFP expression in cortical neurons in vivo (Dittgen et al. 2004).

Not only the resident brain cells but also foreign cells such as tumor or immune cells can be lenti- or retrovirally stably transduced, antibiotically selected and/or sorted by fluorescence-activated cell selection and imaged at later time points in vivo (see below). Like cytoplasmic localization of fluorophores, this method again offers the opportunity selectively to label cell organelles, such as nuclei, e.g., by transfection with an H2B-GFP vector (Yamauchi et al. 2006; Fig. 4, Supplementary video 5; also see below). The imaging of other cell organelles, such as mitochondria, liposomes, or spines in dendrites of neurons opens ways to investigate even subcellular processes by MPLSM.

Of note, some groups have managed to establish in vivo immunostaining techniques, e.g., by intravenous injection of fluorescently labeled antibodies against vascular cell adhesion molecules (Sipkins et al. 2005), which are accessible via the blood stream. Intravenous injection of fluorescently labeled dextrans is an easy way to label the vasculature and provides orientation for imaging structures and cells over a long period of time. It also opens up the study of angiogenesis, vascular regression, blood flow, flux hematocrit, shear rate and microvascular permeability at high resolution (Brown et al. 2001; Chae et al. 2010; Kamoun et al. 2010; von Baumgarten et al. 2011). In addition to these important vascular physiological parameters, attempts have been made to measure other physiological paramters such as hypoxia (Kasischke et al. 2011) and pH (Tantama et al. 2011) by in vivo MPLSM.

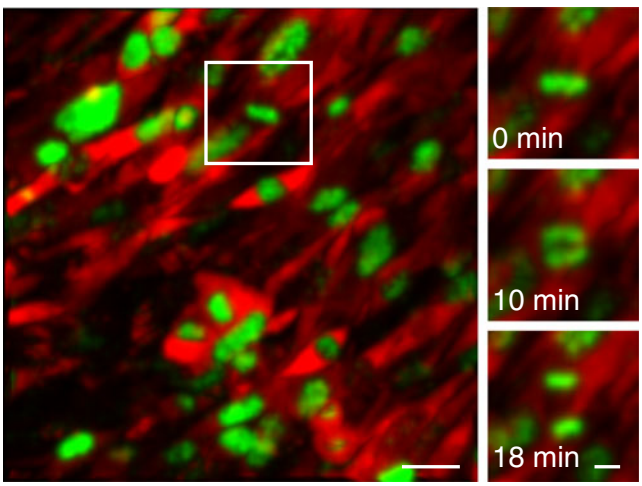

Fig. 4 Tumor cell proliferation and migration. Proliferation of Lewis lung cancer cells in the living brain as revealed by H2B-GFP lentivirus transfection. *Left* Red fluorescent protein (dsRed)-labeled cancer cells (*red*) can be seen with *green* (H2B)-labeled nuclei. This technique enables single cells to be followed over time (see also Supplementary video 5) and detects dividing cells. *Right* Time course of mitosis in the *boxed* cell *left*. M. Osswald, unpublished. *Bars* 30 μm (*left*), 15 μm (*right*)

One important molecular parameter is the change in intracellular calcium. Calcium as a second messenger is a key regulator of many processes including gene expression and is often used as a surrogate parameter for cell–cell communication ("calcium waves") in the central nervous system (Berridge 1993; Leybaert and Sanderson 2012). Whereas in the past, electrophysiology was seen as the main tool for studying intercellular communication, calcium imaging is increasingly playing an equal role in the study of cell circuits. Chemical and genetic calcium sensors can be used for this purpose (see below; Hoogland et al. 2009; Stosiek et al. 2003; Wang et al. 2006). Moreover, the expression of specific genes can be monitored via the expression of fluorescent proteins under the control of the gene promotor (Brown et al. 2001; Fukumura et al. 1998). Although this has not been used frequently for in vivo MPLSM yet, we see this technology as a highly promising avenue of research for studying the role of candidate genes with respect to their function in cell–cell interactions and in crucial physiological changes.

Cell-to-cell communication in health and disease

Cell-to-cell communication can be detected by the spatial proximity of various cell types, by their movement pattern over time (Bartholomaus et al. 2009) and by other parameters such as calcium waves or the transfer of nuclear material (e.g., via phagocytosis). First, resident brain cells communicate with each other. Microglial cells patrol the brain parenchyma (Fig. 2; Nimmerjahn et al. 2005) so that they can take immediate action when a stimulus reaches them. For example, after lasering a single microglial cell, an orchestrated simultaneous reaction of the neighboring microglial cells occurs (Fig. 1, Supplementary video 1). Such a microglial reaction has been shown to be mediated via ATP (Davalos et al. 2005). The in vivo interaction of microglial cells with other brain cells has been demonstrated for many brain pathologies, such as Alzheimer's disease (Fuhrmann et al. 2010). Although astrocytes seem to be immobile cells compared with the patrolling microglial cells (Fig. 2, Supplementary video 3), they communicate with each other via gap junctions in the neocortex (Haas et al. 2006). Calcium signals in astrocytes can reflect a spontaneous activity (Fig. 3, Supplementary video 4; Hirase et al. 2004) or an extrinsic stimulus, e.g., sensory stimulation (Wang et al. 2006). Astrocytic calcium waves can be found between different astrocytes but a correlation has also been observed between neuronal and astrocytic activity (Winship et al. 2007). Under pathological conditions, calcium signals exhibit a transient increase, e.g., after photothrombosis-

induced ischemia (Ding et al. 2009). Likewise, astrocytic synchronous hyperactivity can be detected in a mouse model of Alzheimer's disease (Kuchibhotla et al. 2009). Two-photon imaging has greatly contributed to the understanding of calcium communication in health and disease, as it provides an unprecedented opportunity to image calcium communication in vivo. However, caution has to be taken with regard to the experimental procedure, as the laser itself can manipulate calcium activity dependent on the laser power (Kuga et al. 2011; Wang et al. 2006) and the anesthesia of the studied animal can interfere in the calcium waves (Adelsberger et al. 2005).

In addition, not only normal host cells but also tumor cells can be labeled and their interactions followed over time: for example, after heart or carotid artery injection in brain metastasis studies (Kienast et al. 2010) or after the stereotactic injection of glioma cells for brain tumor studies (von Baumgarten et al. 2011; Winkler et al. 2004, 2009). In the second case, the cover-glass can be removed and re-glued. Figure 4 and Supplementary video 5 give an example of the way that the injection of both H2B-GFP- and RFP-expressing tumor cells (with a red cytoplasm and a green nucleus) can help to identify single tumor cells in a tumor bulk with many densely packed cells. This aids in the determination of the cell number, cell division and cell motility (Fig. 4, Supplementary video 5). The interaction of tumor cells with the microenvironment in the brain is of great interest and invasion of tumor cells into the brain as one common feature of glioma growth is attributable to a complex interaction and communication with the natural brain cells and cerebral microvessels (Winkler et al. 2009).

Cell-and-blood-vessel interaction in health and disease

A large and evolving field of research is the interaction of astrocytes with blood vessels. These glial cells are today considered to be an important regulator of the cerebral blood flow (Attwell et al. 2010; Koehler et al. 2009). To address the role of astrocytic controlled blood flow, Takana and colleagues have used two-photon imaging and photolysis of caged calcium in the GFAP-GFP mouse (Takano et al. 2007a). The photolysis of calcium is followed by a 37% increase in blood flow. Astrocytes are also an essential part of the blood-brain barrier, which is a structure of paramount importance for brain (patho)physiology that can be effectively studied by in vivo MPLSM (Hirase 2005). The blood-brain barrier is also one of the main reasons that systemic therapeutics fail to reach brain pathologies; in glioma, the breakdown of the blood-brain barrier can be imaged over time and quantified by using two-photon microscopy (von Baumgarten et al. 2011). With this technology, we have revealed that a complex and reciprocal interaction of cancer cells and cerebral blood vessels drives tumor initiation, progression and the response to therapies (Kienast et al. 2010; von Baumgarten et al. 2011; Winkler et al. 2004, 2009). One example of the advantages of high-resolution intravital imaging to study of the interaction of single glioma cells with cerebral blood vessels is given in Fig. 5 and Supplementary video 6. In Fig. 6, an example is given of the way that in vivo MPLSM of the very same cancer cells and their adjacent blood vessels over 51 days has provided novel insights into the crucial steps of the formation of brain metastases. All four mandatory steps involve close cancer-cell-blood-vessel interactions (Kienast et al. 2010).

Summary and outlook

In vivo MPLSM of the live brain has already dramatically increased our knowledge about brain function and diseases. In this review, we have tried to demonstrate that this method provides a unique chance to gain novel insights into cell–cell and cell–matrix communication, extending far beyond the field of neuroscience. In the next few years, recent and novel technological developments, both in hardware and fluorescent reporter systems, will increase the experimental opportunities provided by in vivo MPLSM. This includes (with the relevant abbreviations): (1) optical parametric oscillator (OPO) laser technology allowing the excitation of fluorophores to the far-red, while offering increased depth penetration; (2) the smart use of the laser beam to activate

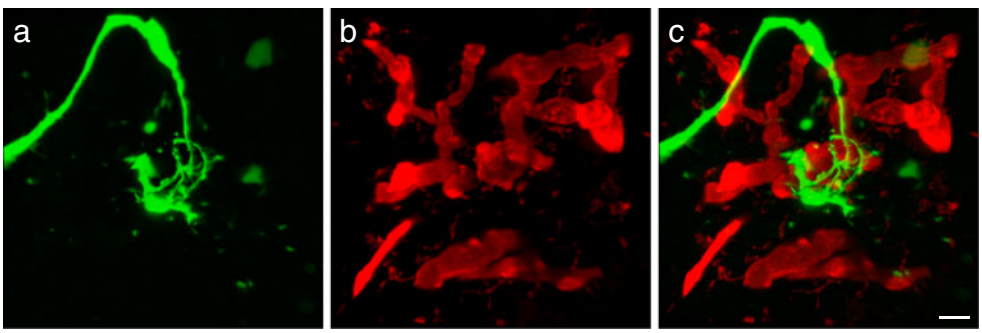

Fig. 5 Glioma-cell–blood-vessel interaction. A glioma cell (*green* in **a**, **c**) is massively surrounding and deforming a dilated angiogenic blood vessel (*red* in **b**, **c**) via a thin (sub-micron) cellular protrusion. M. Osswald, unpublished. *Bar* 20 μm

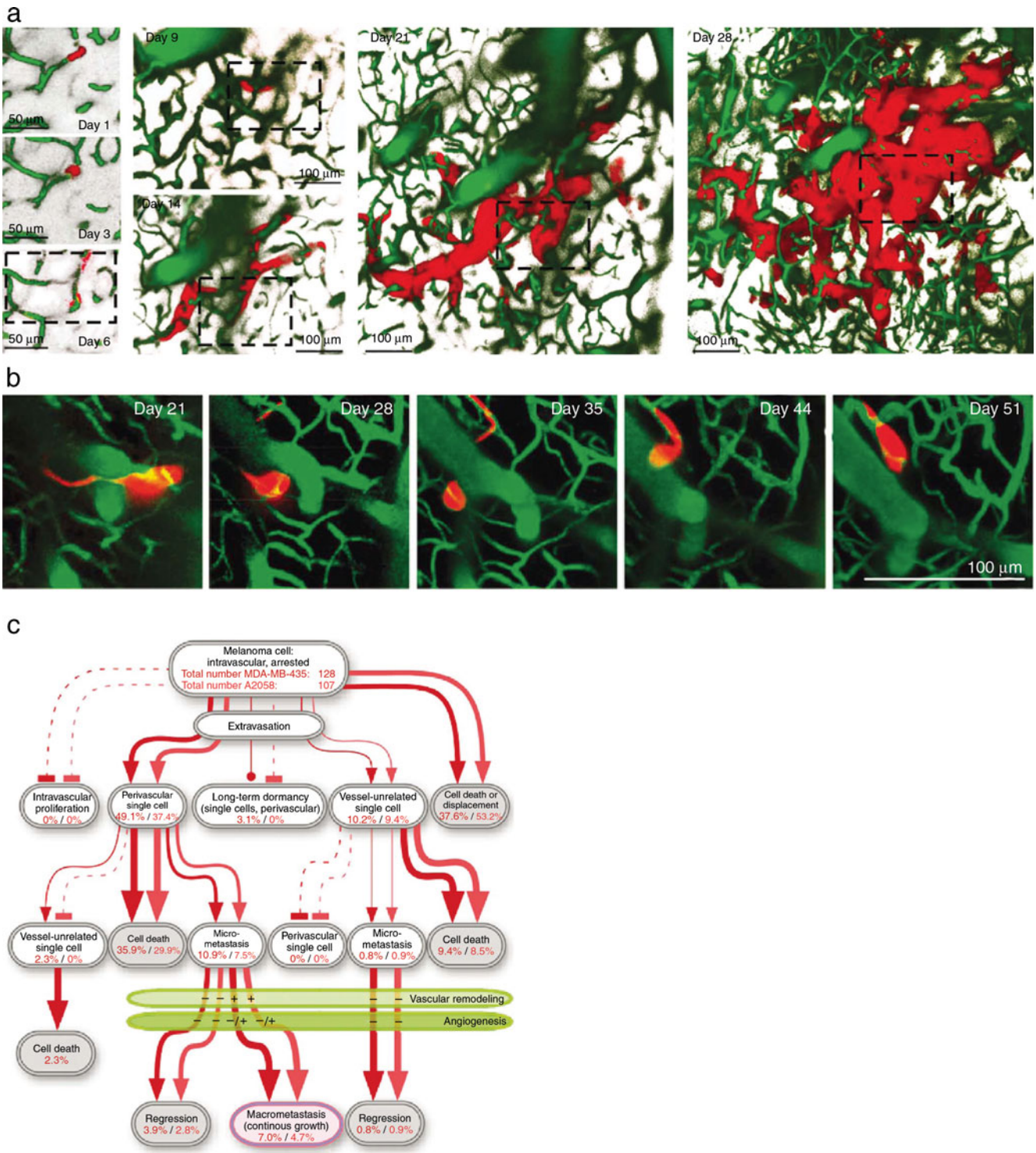

Fig. 6 Single steps of melanoma brain metastasis formation. The opportunity to follow single metastasizing cancer cells in the brain over many weeks provides novel insights into the crucial steps of organ metastasis formation. **a** Successful arrest, extravasation and proliferation by vessel co-option of an A2058 melanoma cell over 28 days. The *box* marks the same region over time (three-dimensional reconstruction; depth: 200–280 µm). **b** Long-term dormancy of an extravasated MDA-MB-435 melanoma cell in a strictly perivascular position. A single melanoma cell does not proliferate but moves along several blood vessels over time, following its own invadopodium. Total distance in three dimensions: 150 µm; depth: 80–230 µm. **c** Quantification of the fate of >100 distinct MDA-MB-435 and A2058 melanoma cells, as traced over many weeks. Note the essential, efficient and inefficient steps of brain metastasis formation and the dead ends. The percentages represent the fraction of the initially arrested tumor cells of the indicated cell lines. From: Kienast et al. (2010)

regions selectively, as with local activation of fluorescent molecular probes (LAMP), which has been shown to work for two-photon imaging, where it has been used to study gap junction communication between cells (Dakin and Li 2006); (3) the study of protein–protein interactions by fluorescence resonance energy transfer (FRET)/fluorescence lifetime imaging microscopy (FLIM); (4) photoactivatable fluorophores that permit selective intravital marking of single cells or intracellular regions (Niesner and Hauser 2011); (5) the development of additional genetic systems for the imaging of gene expression and intracellular metabolism.

References

Adelsberger H, Garaschuk O, Konnerth A (2005) Cortical calcium waves in resting newborn mice. Nat Neurosci 8:988–990

Attwell D, Buchan AM, Charpak S, Lauritzen M, Macvicar BA, Newman EA (2010) Glial and neuronal control of brain blood flow. Nature 468:232–243

Barretto RP, Ko TH, Jung JC, Wang TJ, Capps G, Waters AC, Ziv Y, Attardo A, Recht L, Schnitzer MJ (2011) Time-lapse imaging of disease progression in deep brain areas using fluorescence microendoscopy. Nat Med 17:223–228

Bartholomaus I, Kawakami N, Odoardi F, Schlager C, Miljkovic D, Ellwart JW, Klinkert WE, Flugel-Koch C, Issekutz TB, Wekerle H, Flugel A (2009) Effector T cell interactions with meningeal vascular structures in nascent autoimmune CNS lesions. Nature 462:94–98

Berridge MJ (1993) Inositol trisphosphate and calcium signalling. Nature 361:315–325

Brown EB, Campbell RB, Tsuzuki Y, Xu L, Carmeliet P, Fukumura D, Jain RK (2001) In vivo measurement of gene expression, angiogenesis and physiological function in tumors using multiphoton laser scanning microscopy. Nat Med 7:864–868

Brown E, McKee T, di Tomaso E, Pluen A, Seed B, Boucher Y, Jain RK (2003) Dynamic imaging of collagen and its modulation in tumors in vivo using second-harmonic generation. Nat Med 9:796–800

Chae SS, Kamoun WS, Farrar CT, Kirkpatrick ND, Niemeyer E, de Graaf AM, Sorensen AG, Munn LL, Jain RK, Fukumura D (2010) Angiopoietin-2 interferes with anti-VEGFR2-induced vessel normalization and survival benefit in mice bearing gliomas. Clin Cancer Res 16:3618–3627

Dakin K, Li WH (2006) Infrared-LAMP: two-photon uncaging and imaging of gap junctional communication in three dimensions. Nat Methods 3:959

Davalos D, Grutzendler J, Yang G, Kim JV, Zuo Y, Jung S, Littman DR, Dustin ML, Gan WB (2005) ATP mediates rapid microglial response to local brain injury in vivo. Nat Neurosci 8:752–758

Denk W, Strickler JH, Webb WW (1990) Two-photon laser scanning fluorescence microscopy. Science 248:73–76

Ding S, Wang T, Cui W, Haydon PG (2009) Photothrombosis ischemia stimulates a sustained astrocytic Ca^{2+} signaling in vivo. Glia 57:767–776

Dittgen T, Nimmerjahn A, Komai S, Licznerski P, Waters J, Margrie TW, Helmchen F, Denk W, Brecht M, Osten P (2004) Lentivirus-based genetic manipulations of cortical neurons and their optical and electrophysiological monitoring in vivo. Proc Natl Acad Sci USA 101:18206–18211

Drobizhev M, Makarov NS, Tillo SE, Hughes TE, Rebane A (2011) Two-photon absorption properties of fluorescent proteins. Nat Methods 8:393–399

Feng G, Mellor RH, Bernstein M, Keller-Peck C, Nguyen QT, Wallace M, Nerbonne JM, Lichtman JW, Sanes JR (2000) Imaging neuronal subsets in transgenic mice expressing multiple spectral variants of GFP. Neuron 28:41–51

Fuhrmann M, Mitteregger G, Kretzschmar H, Herms J (2007) Dendritic pathology in prion disease starts at the synaptic spine. J Neurosci 27:6224–6233

Fuhrmann M, Bittner T, Jung CK, Burgold S, Page RM, Mitteregger G, Haass C, LaFerla FM, Kretzschmar H, Herms J (2010) Microglial Cx3cr1 knockout prevents neuron loss in a mouse model of Alzheimer's disease. Nat Neurosci 13:411–413

Fukumura D, Xavier R, Sugiura T, Chen Y, Park EC, Lu N, Selig M, Nielsen G, Taksir T, Jain RK, Seed B (1998) Tumor induction of VEGF promoter activity in stromal cells. Cell 94:715–725

Gee KR, Brown KA, Chen WN, Bishop-Stewart J, Gray D, Johnson I (2000) Chemical and physiological characterization of fluo-4 Ca(2+)-indicator dyes. Cell Calcium 27:97–106

Gobel W, Kampa BM, Helmchen F (2007) Imaging cellular network dynamics in three dimensions using fast 3D laser scanning. Nat Methods 4:73–79

Grewe BF, Langer D, Kasper H, Kampa BM, Helmchen F (2010) High-speed in vivo calcium imaging reveals neuronal network activity with near-millisecond precision. Nat Methods 7:399–405

Haas B, Schipke CG, Peters O, Sohl G, Willecke K, Kettenmann H (2006) Activity-dependent ATP-waves in the mouse neocortex are independent from astrocytic calcium waves. Cereb Cortex 16:237–246

Hefendehl JK, Wegenast-Braun BM, Liebig C, Eicke D, Milford D, Calhoun ME, Kohsaka S, Eichner M, Jucker M (2011) Long-term in vivo imaging of beta-amyloid plaque appearance and growth in a mouse model of cerebral beta-amyloidosis. J Neurosci 31:624–629

Helmchen F, Denk W (2005) Deep tissue two-photon microscopy. Nat Methods 2:932–940

Hirase H (2005) A multi-photon window onto neuronal-glial-vascular communication. Trends Neurosci 28:217–219

Hirase H, Qian L, Bartho P, Buzsaki G (2004) Calcium dynamics of cortical astrocytic networks in vivo. PLoS Biol 2:E96

Hoogland TM, Kuhn B, Gobel W, Huang W, Nakai J, Helmchen F, Flint J, Wang SS (2009) Radially expanding transglial calcium waves in the intact cerebellum. Proc Natl Acad Sci USA 106:3496–3501

Jung S, Aliberti J, Graemmel P, Sunshine MJ, Kreutzberg GW, Sher A, Littman DR (2000) Analysis of fractalkine receptor CX(3)CR1 function by targeted deletion and green fluorescent protein reporter gene insertion. Mol Cell Biol 20:4106–4114

Kamoun WS, Chae SS, Lacorre DA, Tyrrell JA, Mitre M, Gillissen MA, Fukumura D, Jain RK, Munn LL (2010) Simultaneous measurement of RBC velocity, flux, hematocrit and shear rate in vascular networks. Nat Methods 7:655–660

Kantevari S, Matsuzaki M, Kanemoto Y, Kasai H, Ellis-Davies GC (2010) Two-color, two-photon uncaging of glutamate and GABA. Nat Methods 7:123–125

Kasischke KA, Vishwasrao HD, Fisher PJ, Zipfel WR, Webb WW (2004) Neural activity triggers neuronal oxidative metabolism followed by astrocytic glycolysis. Science 305:99–103

Kasischke KA, Lambert EM, Panepento B, Sun A, Gelbard HA, Burgess RW, Foster TH, Nedergaard M (2011) Two-photon NADH imaging exposes boundaries of oxygen diffusion in cortical vascular supply regions. J Cereb Blood Flow Metab 31:68–81

Kawakami N, Nagerl UV, Odoardi F, Bonhoeffer T, Wekerle H, Flugel A (2005) Live imaging of effector cell trafficking and autoantigen

recognition within the unfolding autoimmune encephalomyelitis lesion. J Exp Med 201:1805–1814
Kedrin D, Gligorijevic B, Wyckoff J, Verkhusha VV, Condeelis J, Segall JE, van Rheenen J (2008) Intravital imaging of metastatic behavior through a mammary imaging window. Nat Methods 5:1019–1021
Kienast Y, von Baumgarten L, Fuhrmann M, Klinkert WE, Goldbrunner R, Herms J, Winkler F (2010) Real-time imaging reveals the single steps of brain metastasis formation. Nat Med 16:116–122
Koehler RC, Roman RJ, Harder DR (2009) Astrocytes and the regulation of cerebral blood flow. Trends Neurosci 32:160–169
Kuchibhotla KV, Lattarulo CR, Hyman BT, Bacskai BJ (2009) Synchronous hyperactivity and intercellular calcium waves in astrocytes in Alzheimer mice. Science 323:1211–1215
Kuga N, Sasaki T, Takahara Y, Matsuki N, Ikegaya Y (2011) Large-scale calcium waves traveling through astrocytic networks in vivo. J Neurosci 31:2607–2614
Leybaert L, Sanderson MJ (2012) Intercellular Ca(2+) waves: mechanisms and function. Physiol Rev 92:1359–1392
Misgeld T, Kerschensteiner M, Bareyre FM, Burgess RW, Lichtman JW (2007) Imaging axonal transport of mitochondria in vivo. Nat Methods 4:559–561
Motoike T, Loughna S, Perens E, Roman BL, Liao W, Chau TC, Richardson CD, Kawate T, Kuno J, Weinstein BM et al (2000) Universal GFP reporter for the study of vascular development. Genesis 28:75–81
Nagayama S, Zeng S, Xiong W, Fletcher ML, Masurkar AV, Davis DJ, Pieribone VA, Chen WR (2007) In vivo simultaneous tracing and Ca(2+) imaging of local neuronal circuits. Neuron 53:789–803
Niesner RA, Hauser AE (2011) Recent advances in dynamic intravital multi-photon microscopy. Cytometry A 79:789–798
Nimmerjahn A, Kirchhoff F, Kerr JN, Helmchen F (2004) Sulforhodamine 101 as a specific marker of astroglia in the neocortex in vivo. Nat Methods 1:31–37
Nimmerjahn A, Kirchhoff F, Helmchen F (2005) Resting microglial cells are highly dynamic surveillants of brain parenchyma in vivo. Science 308:1314–1318
Nolte C, Matyash M, Pivneva T, Schipke CG, Ohlemeyer C, Hanisch UK, Kirchhoff F, Kettenmann H (2001) GFAP promoter-controlled EGFP-expressing transgenic mice: a tool to visualize astrocytes and astrogliosis in living brain tissue. Glia 33:72–86
Sipkins DA, Wei X, Wu JW, Runnels JM, Cote D, Means TK, Luster AD, Scadden DT, Lin CP (2005) In vivo imaging of specialized bone marrow endothelial microdomains for tumour engraftment. Nature 435:969–973
Squirrell JM, Wokosin DL, White JG, Bavister BD (1999) Long-term two-photon fluorescence imaging of mammalian embryos without compromising viability. Nat Biotechnol 17:763–767
Stosiek C, Garaschuk O, Holthoff K, Konnerth A (2003) In vivo two-photon calcium imaging of neuronal networks. Proc Natl Acad Sci USA 100:7319–7324
Svoboda K, Tank DW, Denk W (1996) Direct measurement of coupling between dendritic spines and shafts. Science 272:716–719
Takano T, Han X, Deane R, Zlokovic B, Nedergaard M (2007a) Two-photon imaging of astrocytic Ca^{2+} signaling and the microvasculature in experimental mice models of Alzheimer's disease. Ann N Y Acad Sci 1097:40–50
Takano T, Tian GF, Peng W, Lou N, Lovatt D, Hansen AJ, Kasischke KA, Nedergaard M (2007b) Cortical spreading depression causes and coincides with tissue hypoxia. Nat Neurosci 10:754–762
Tantama M, Hung YP, Yellen G (2011) Imaging intracellular pH in live cells with a genetically encoded red fluorescent protein sensor. J Am Chem Soc 133:10034–10037
Tatenhorst L, Puttmann S, Senner V, Paulus W (2005) Genes associated with fast glioma cell migration in vitro and in vivo. Brain Pathol 15:46–54
Tong RT, Boucher Y, Kozin SV, Winkler F, Hicklin DJ, Jain RK (2004) Vascular normalization by vascular endothelial growth factor receptor 2 blockade induces a pressure gradient across the vasculature and improves drug penetration in tumors. Cancer Res 64:3731–3736
von Baumgarten L, Brucker D, Tirniceru A, Kienast Y, Grau S, Burgold S, Herms J, Winkler F (2011) Bevacizumab has differential and dose-dependent effects on glioma blood vessels and tumor cells. Clin Cancer Res 17:6192–6205
Wang X, Lou N, Xu Q, Tian GF, Peng WG, Han X, Kang J, Takano T, Nedergaard M (2006) Astrocytic Ca^{2+} signaling evoked by sensory stimulation in vivo. Nat Neurosci 9:816–823
Winkler F, Kozin SV, Tong RT, Chae SS, Booth MF, Garkavtsev I, Xu L, Hicklin DJ, Fukumura D, di Tomaso E et al (2004) Kinetics of vascular normalization by VEGFR2 blockade governs brain tumor response to radiation: role of oxygenation, angiopoietin-1, and matrix metalloproteinases. Cancer Cell 6:553–563
Winkler F, Kienast Y, Fuhrmann M, von Baumgarten L, Burgold S, Mitteregger G, Kretzschmar H, Herms J (2009) Imaging glioma cell invasion in vivo reveals mechanisms of dissemination and peritumoral angiogenesis. Glia 57:1306–1315
Winship IR, Plaa N, Murphy TH (2007) Rapid astrocyte calcium signals correlate with neuronal activity and onset of the hemodynamic response in vivo. J Neurosci 27:6268–6272
Wood S (1958) Pathogenesis of metastasis formation observed in vivo in the rabbit ear chamber. AMA Arch Pathol 66:550–568
Xu HT, Pan F, Yang G, Gan WB (2007) Choice of cranial window type for in vivo imaging affects dendritic spine turnover in the cortex. Nat Neurosci 10:549–551
Yamauchi K, Yang M, Jiang P, Xu M, Yamamoto N, Tsuchiya H, Tomita K, Moossa AR, Bouvet M, Hoffman RM (2006) Development of real-time subcellular dynamic multicolor imaging of cancer-cell trafficking in live mice with a variable-magnification whole-mouse imaging system. Cancer Res 66:4208–4214
Yuan F, Salehi HA, Boucher Y, Vasthare US, Tuma RF, Jain RK (1994) Vascular permeability and microcirculation of gliomas and mammary carcinomas transplanted in rat and mouse cranial windows. Cancer Res 54:4564–4568
Yuan F, Chen Y, Dellian M, Safabakhsh N, Ferrara N, Jain RK (1996) Time-dependent vascular regression and permeability changes in established human tumor xenografts induced by an anti-vascular endothelial growth factor/vascular permeability factor antibody. Proc Natl Acad Sci USA 93:14765–14770